Search for Doubly-Charged Higgs Bosons Decaying to Dileptons in $p\bar{p}$ Collisions at $\sqrt{s}$=1.96 TeV

D. Acosta,[16] T. Affolder,[9] T. Akimoto,[54] M.G. Albrow,[15] D. Ambrose,[43] S. Amerio,[42] D. Amidei,[33] A. Anastassov,[50] K. Anikeev,[31] A. Annovi,[44] J. Antos,[1] M. Aoki,[54] G. Apollinari,[15] T. Arisawa,[56] J-F. Arguin,[32] A. Artikov,[13] W. Ashmanskas,[2] A. Attal,[7] F. Azfar,[41] P. Azzi-Bacchetta,[42] N. Bacchetta,[42] H. Bachacou,[28] W. Badgett,[15] A. Barbaro-Galtieri,[28] G.J. Barker,[25] V.E. Barnes,[46] B.A. Barnett,[24] S. Baroiant,[6] M. Barone,[17] G. Bauer,[31] F. Bedeschi,[44] S. Behari,[24] S. Belforte,[53] G. Bellettini,[44] J. Bellinger,[58] D. Benjamin,[14] A. Beretvas,[15] A. Bhatti,[48] M. Binkley,[15] D. Bisello,[42] M. Bishai,[15] R.E. Blair,[2] C. Blocker,[5] K. Bloom,[33] B. Blumenfeld,[24] A. Bocci,[48] A. Bodek,[47] G. Bolla,[46] A. Bolshov,[31] P.S.L. Booth,[29] D. Bortoletto,[46] J. Boudreau,[45] S. Bourov,[15] C. Bromberg,[34] E. Brubaker,[28] J. Budagov,[13] H.S. Budd,[47] K. Burkett,[15] G. Busetto,[42] P. Bussey,[19] K.L. Byrum,[2] S. Cabrera,[14] P. Calafiura,[28] M. Campanelli,[18] M. Campbell,[33] A. Canepa,[46] M. Casarsa,[53] D. Carlsmith,[58] S. Carron,[14] R. Carosi,[44] M. Cavalli-Sforza,[3] A. Castro,[4] P. Catastini,[44] D. Cauz,[53] A. Cerri,[28] C. Cerri,[44] L. Cerrito,[23] J. Chapman,[33] C. Chen,[43] Y.C. Chen,[1] M. Chertok,[6] G. Chiarelli,[44] G. Chlachidze,[13] F. Chlebana,[15] I. Cho,[27] K. Cho,[27] D. Chokheli,[13] M.L. Chu,[1] S. Chuang,[58] J.Y. Chung,[38] W-H. Chung,[58] Y.S. Chung,[47] C.I. Ciobanu,[23] M.A. Ciocci,[44] A.G. Clark,[18] D. Clark,[5] M. Coca,[47] A. Connolly,[28] M. Convery,[48] J. Conway,[50] B. Cooper,[30] M. Cordelli,[17] G. Cortiana,[42] J. Cranshaw,[52] J. Cuevas,[10] R. Culbertson,[15] C. Currat,[28] D. Cyr,[58] D. Dagenhart,[5] S. Da Ronco,[42] S. D'Auria,[19] P. de Barbaro,[47] S. De Cecco,[49] G. De Lentdecker,[47] S. Dell'Agnello,[17] M. Dell'Orso,[44] S. Demers,[47] L. Demortier,[48] M. Deninno,[4] D. De Pedis,[49] P.F. Derwent,[15] C. Dionisi,[49] J.R. Dittmann,[15] P. Doksus,[23] A. Dominguez,[28] S. Donati,[44] M. Donega,[18] J. Donini,[42] M. D'Onofrio,[18] T. Dorigo,[42] V. Drollinger,[36] K. Ebina,[56] N. Eddy,[23] R. Ely,[28] R. Erbacher,[15] M. Erdmann,[25] D. Errede,[23] S. Errede,[23] R. Eusebi,[47] H-C. Fang,[28] S. Farrington,[29] I. Fedorko,[44] R.G. Feild,[59] M. Feindt,[25] J.P. Fernandez,[46] C. Ferretti,[33] R.D. Field,[16] I. Fiori,[44] G. Flanagan,[34] B. Flaugher,[15] L.R. Flores-Castillo,[45] A. Foland,[20] S. Forrester,[6] G.W. Foster,[15] M. Franklin,[20] J. Freeman,[28] H. Frisch,[12] Y. Fujii,[26] I. Furic,[31] A. Gajjar,[29] A. Gallas,[37] J. Galyardt,[11] M. Gallinaro,[48] M. Garcia-Sciveres,[28] A.F. Garfinkel,[46] C. Gay,[59] H. Gerberich,[14] D.W. Gerdes,[33] E. Gerchtein,[11] S. Giagu,[49] P. Giannetti,[44] A. Gibson,[28] K. Gibson,[11] C. Ginsburg,[58] K. Giolo,[46] M. Giordani,[53] G. Giurgiu,[11] V. Glagolev,[13] D. Glenzinski,[15] M. Gold,[36] N. Goldschmidt,[33] D. Goldstein,[7] J. Goldstein,[41] G. Gomez,[10] G. Gomez-Ceballos,[31] M. Goncharov,[51] O. González,[46] I. Gorelov,[36] A.T. Goshaw,[14] Y. Gotra,[45] K. Goulianos,[48] A. Gresele,[4] C. Grosso-Pilcher,[12] M. Guenther,[46] J. Guimaraes da Costa,[20] C. Haber,[28]

K. Hahn,[43] S.R. Hahn,[15] E. Halkiadakis,[47] R. Handler,[58] F. Happacher,[17] K. Hara,[54] M. Hare,[55] R.F. Harr,[57] R.M. Harris,[15] F. Hartmann,[25] K. Hatakeyama,[48] J. Hauser,[7] C. Hays,[14] H. Hayward,[29] E. Heider,[55] B. Heinemann,[29] J. Heinrich,[43] M. Hennecke,[25] M. Herndon,[24] C. Hill,[9] D. Hirschbuehl,[25] A. Hocker,[47] K.D. Hoffman,[12] A. Holloway,[20] S. Hou,[1] M.A. Houlden,[29] B.T. Huffman,[41] Y. Huang,[14] R.E. Hughes,[38] J. Huston,[34] K. Ikado,[56] J. Incandela,[9] G. Introzzi,[44] M. Iori,[49] Y. Ishizawa,[54] C. Issever,[9] A. Ivanov,[47] Y. Iwata,[22] B. Iyutin,[31] E. James,[15] D. Jang,[50] J. Jarrell,[36] D. Jeans,[49] H. Jensen,[15] E.J. Jeon,[27] M. Jones,[46] K.K. Joo,[27] S. Jun,[11] T. Junk,[23] T. Kamon,[51] J. Kang,[33] M. Karagoz Unel,[37] P.E. Karchin,[57] S. Kartal,[15] Y. Kato,[40] Y. Kemp,[25] R. Kephart,[15] U. Kerzel,[25] V. Khotilovich,[51] B. Kilminster,[38] D.H. Kim,[27] H.S. Kim,[23] J.E. Kim,[27] M.J. Kim,[11] M.S. Kim,[27] S.B. Kim,[27] S.H. Kim,[54] T.H. Kim,[31] Y.K. Kim,[12] B.T. King,[29] M. Kirby,[14] L. Kirsch,[5] S. Klimenko,[16] B. Knuteson,[31] B.R. Ko,[14] H. Kobayashi,[54] P. Koehn,[38] D.J. Kong,[27] K. Kondo,[56] J. Konigsberg,[16] K. Kordas,[32] A. Korn,[31] A. Korytov,[16] K. Kotelnikov,[35] A.V. Kotwal,[14] A. Kovalev,[43] J. Kraus,[23] I. Kravchenko,[31] A. Kreymer,[15] J. Kroll,[43] M. Kruse,[14] V. Krutelyov,[51] S.E. Kuhlmann,[2] N. Kuznetsova,[15] A.T. Laasanen,[46] S. Lai,[32] S. Lami,[48] S. Lammel,[15] J. Lancaster,[14] M. Lancaster,[30] R. Lander,[6] K. Lannon,[38] A. Lath,[50] G. Latino,[36] R. Lauhakangas,[21] I. Lazzizzera,[42] Y. Le,[24] C. Lecci,[25] T. LeCompte,[2] J. Lee,[27] J. Lee,[47] S.W. Lee,[51] N. Leonardo,[31] S. Leone,[44] J.D. Lewis,[15] K. Li,[59] C. Lin,[59] C.S. Lin,[15] M. Lindgren,[15] T.M. Liss,[23] D.O. Litvintsev,[15] T. Liu,[15] Y. Liu,[18] N.S. Lockyer,[43] A. Loginov,[35] M. Loreti,[42] P. Loverre,[49] R-S. Lu,[1] D. Lucchesi,[42] P. Lujan,[28] P. Lukens,[15] L. Lyons,[41] J. Lys,[28] R. Lysak,[1] D. MacQueen,[32] R. Madrak,[20] K. Maeshima,[15] P. Maksimovic,[24] L. Malferrari,[4] G. Manca,[29] R. Marginean,[38] M. Martin,[24] A. Martin,[59] V. Martin,[37] M. Martínez,[3] T. Maruyama,[54] H. Matsunaga,[54] M. Mattson,[57] P. Mazzanti,[4] K.S. McFarland,[47] D. McGivern,[30] P.M. McIntyre,[51] P. McNamara,[50] R. NcNulty,[29] S. Menzemer,[31] A. Menzione,[44] P. Merkel,[15] C. Mesropian,[48] A. Messina,[49] T. Miao,[15] N. Miladinovic,[5] L. Miller,[20] R. Miller,[34] J.S. Miller,[33] R. Miquel,[28] S. Miscetti,[17] G. Mitselmakher,[16] A. Miyamoto,[26] Y. Miyazaki,[40] N. Moggi,[4] B. Mohr,[7] R. Moore,[15] M. Morello,[44] T. Moulik,[46] P.A. Movilla Fernandez,[28] A. Mukherjee,[15] M. Mulhearn,[31] T. Muller,[25] R. Mumford,[24] A. Munar,[43] P. Murat,[15] J. Nachtman,[15] S. Nahn,[59] I. Nakamura,[43] I. Nakano,[39] A. Napier,[55] R. Napora,[24] D. Naumov,[36] V. Necula,[16] F. Niell,[33] J. Nielsen,[28] C. Nelson,[15] T. Nelson,[15] C. Neu,[43] M.S. Neubauer,[8] C. Newman-Holmes,[15] A-S. Nicollerat,[18] T. Nigmanov,[45] L. Nodulman,[2] O. Norniella,[3] K. Oesterberg,[21] T. Ogawa,[56] S.H. Oh,[14] Y.D. Oh,[27] T. Ohsugi,[22] T. Okusawa,[40] R. Oldeman,[49] R. Orava,[21] W. Orejudos,[28] C. Pagliarone,[44] F. Palmonari,[44] R. Paoletti,[44] V. Papadimitriou,[15] S. Pashapour,[32] J. Patrick,[15] G. Pauletta,[53] M. Paulini,[11] T. Pauly,[41] C. Paus,[31] D. Pellett,[6] A. Penzo,[53] T.J. Phillips,[14] G. Piacentino,[44] J. Piedra,[10] K.T. Pitts,[23] C. Plager,[7]

2

A. Pompoš,[46] L. Pondrom,[58] G. Pope,[45] O. Poukhov,[13] F. Prakoshyn,[13] T. Pratt,[29] A. Pronko,[16] J. Proudfoot,[2] F. Ptohos,[17] G. Punzi,[44] J. Rademacker,[41] A. Rakitine,[31] S. Rappoccio,[20] F. Ratnikov,[50] H. Ray,[33] A. Reichold,[41] B. Reisert,[15] V. Rekovic,[36] P. Renton,[41] M. Rescigno,[49] F. Rimondi,[4] K. Rinnert,[25] L. Ristori,[44] W.J. Robertson,[14] A. Robson,[41] T. Rodrigo,[10] S. Rolli,[55] L. Rosenson,[31] R. Roser,[15] R. Rossin,[42] C. Rott,[46] J. Russ,[11] A. Ruiz,[10] D. Ryan,[55] H. Saarikko,[21] A. Safonov,[6] R. St. Denis,[19] W.K. Sakumoto,[47] G. Salamanna,[49] D. Saltzberg,[7] C. Sanchez,[3] A. Sansoni,[17] L. Santi,[53] S. Sarkar,[49] K. Sato,[54] P. Savard,[32] A. Savoy-Navarro,[15] P. Schemitz,[25] P. Schlabach,[15] E.E. Schmidt,[15] M.P. Schmidt,[59] M. Schmitt,[37] L. Scodellaro,[42] A. Scribano,[44] F. Scuri,[44] A. Sedov,[46] S. Seidel,[36] Y. Seiya,[40] F. Semeria,[4] L. Sexton-Kennedy,[15] I. Sfiligoi,[17] M.D. Shapiro,[28] T. Shears,[29] P.F. Shepard,[45] M. Shimojima,[54] M. Shochet,[12] Y. Shon,[58] I. Shreyber,[35] A. Sidoti,[44] J. Siegrist,[28] M. Siket,[1] A. Sill,[52] P. Sinervo,[32] A. Sisakyan,[13] A. Skiba,[25] A.J. Slaughter,[15] K. Sliwa,[55] D. Smirnov,[36] J.R. Smith,[6] F.D. Snider,[15] R. Snihur,[32] S.V. Somalwar,[50] J. Spalding,[15] M. Spezziga,[52] L. Spiegel,[15] F. Spinella,[44] M. Spiropulu,[9] P. Squillacioti,[44] H. Stadie,[25] A. Stefanini,[44] B. Stelzer,[32] O. Stelzer-Chilton,[32] J. Strologas,[36] D. Stuart,[9] A. Sukhanov,[16] K. Sumorok,[31] H. Sun,[55] T. Suzuki,[54] A. Taffard,[23] R. Tafirout,[32] S.F. Takach,[57] H. Takano,[54] R. Takashima,[22] Y. Takeuchi,[54] K. Takikawa,[54] M. Tanaka,[2] R. Tanaka,[39] N. Tanimoto,[39] S. Tapprogge,[21] M. Tecchio,[33] P.K. Teng,[1] K. Terashi,[48] R.J. Tesarek,[15] S. Tether,[31] J. Thom,[15] A.S. Thompson,[19] E. Thomson,[43] P. Tipton,[47] V. Tiwari,[11] S. Tkaczyk,[15] D. Toback,[51] K. Tollefson,[34] T. Tomura,[54] D. Tonelli,[44] M. Tönnesmann,[34] S. Torre,[44] D. Torretta,[15] W. Trischuk,[32] J. Tseng,[41] R. Tsuchiya,[56] S. Tsuno,[39] D. Tsybychev,[16] N. Turini,[44] M. Turner,[29] F. Ukegawa,[54] T. Unverhau,[19] S. Uozumi,[54] D. Usynin,[43] L. Vacavant,[28] A. Vaiciulis,[47] A. Varganov,[33] E. Vataga,[44] S. Vejcik III,[15] G. Velev,[15] G. Veramendi,[23] T. Vickey,[23] R. Vidal,[15] I. Vila,[10] R. Vilar,[10] I. Volobouev,[28] M. von der Mey,[7] R.G. Wagner,[2] R.L. Wagner,[15] W. Wagner,[25] R. Wallny,[7] T. Walter,[25] T. Yamashita,[39] K. Yamamoto,[40] Z. Wan,[50] M.J. Wang,[1] S.M. Wang,[16] A. Warburton,[32] B. Ward,[19] S. Waschke,[19] D. Waters,[30] T. Watts,[50] M. Weber,[28] W.C. Wester III,[15] B. Whitehouse,[55] A.B. Wicklund,[2] E. Wicklund,[15] H.H. Williams,[43] P. Wilson,[15] B.L. Winer,[38] P. Wittich,[43] S. Wolbers,[15] M. Wolter,[55] M. Worcester,[7] S. Worm,[50] T. Wright,[33] X. Wu,[18] F. Würthwein,[8] A. Wyatt,[30] A. Yagil,[15] U.K. Yang,[12] W. Yao,[28] G.P. Yeh,[15] K. Yi,[24] J. Yoh,[15] P. Yoon,[47] K. Yorita,[56] T. Yoshida,[40] I. Yu,[27] S. Yu,[43] Z. Yu,[59] J.C. Yun,[15] L. Zanello,[49] A. Zanetti,[53] I. Zaw,[20] F. Zetti,[44] J. Zhou,[50] A. Zsenei,[18] and S. Zucchelli,[4]

(CDF Collaboration)

[1] *Institute of Physics, Academia Sinica, Taipei, Taiwan 11529, Republic of China*

3

[2] *Argonne National Laboratory, Argonne, Illinois 60439*

[3] *Institut de Fisica d'Altes Energies, Universitat Autonoma de Barcelona, E-08193, Bellaterra (Barcelona), Spain*

[4] *Istituto Nazionale di Fisica Nucleare, University of Bologna, I-40127 Bologna, Italy*

[5] *Brandeis University, Waltham, Massachusetts 02254*

[6] *University of California at Davis, Davis, California 95616*

[7] *University of California at Los Angeles, Los Angeles, California 90024*

[8] *University of California at San Diego, La Jolla, California 92093*

[9] *University of California at Santa Barbara, Santa Barbara, California 93106*

[10] *Instituto de Fisica de Cantabria, CSIC-University of Cantabria, 39005 Santander, Spain*

[11] *Carnegie Mellon University, Pittsburgh, PA 15213*

[12] *Enrico Fermi Institute, University of Chicago, Chicago, Illinois 60637*

[13] *Joint Institute for Nuclear Research, RU-141980 Dubna, Russia*

[14] *Duke University, Durham, North Carolina 27708*

[15] *Fermi National Accelerator Laboratory, Batavia, Illinois 60510*

[16] *University of Florida, Gainesville, Florida 32611*

[17] *Laboratori Nazionali di Frascati, Istituto Nazionale di Fisica Nucleare, I-00044 Frascati, Italy*

[18] *University of Geneva, CH-1211 Geneva 4, Switzerland*

[19] *Glasgow University, Glasgow G12 8QQ, United Kingdom*

[20] *Harvard University, Cambridge, Massachusetts 02138*

[21] *The Helsinki Group: Helsinki Institute of Physics; and Division of High Energy Physics, Department of Physical Sciences, University of Helsinki, FIN-00044, Helsinki, Finland*

[22] *Hiroshima University, Higashi-Hiroshima 724, Japan*

[23] *University of Illinois, Urbana, Illinois 61801*

[24] *The Johns Hopkins University, Baltimore, Maryland 21218*

[25] *Institut für Experimentelle Kernphysik, Universität Karlsruhe, 76128 Karlsruhe, Germany*

[26] *High Energy Accelerator Research Organization (KEK), Tsukuba, Ibaraki 305, Japan*

[27] *Center for High Energy Physics: Kyungpook National University, Taegu 702-701; Seoul National University, Seoul 151-742; and SungKyunKwan University, Suwon 440-746; Korea*

[28] *Ernest Orlando Lawrence Berkeley National Laboratory, Berkeley, California 94720*

[29] *University of Liverpool, Liverpool L69 7ZE, United Kingdom*

[30] *University College London, London WC1E 6BT, United Kingdom*

[31] *Massachusetts Institute of Technology, Cambridge, Massachusetts 02139*

[32] *Institute of Particle Physics, McGill University, Montréal, Canada H3A 2T8; and University of Toronto, Toronto, Canada M5S 1A7*

[33] *University of Michigan, Ann Arbor, Michigan 48109*

[34] *Michigan State University, East Lansing, Michigan 48824*

[35] *Institution for Theoretical and Experimental Physics, ITEP, Moscow 117259, Russia*

[36] *University of New Mexico, Albuquerque, New Mexico 87131*

[37] *Northwestern University, Evanston, Illinois 60208*

[38] *The Ohio State University, Columbus, Ohio 43210*

[39] *Okayama University, Okayama 700-8530, Japan*

[40] *Osaka City University, Osaka 588, Japan*

[41] *University of Oxford, Oxford OX1 3RH, United Kingdom*

[42] *University of Padova, Istituto Nazionale di Fisica Nucleare, Sezione di Padova-Trento, I-35131 Padova, Italy*

[43] *University of Pennsylvania, Philadelphia, Pennsylvania 19104*

[44] *Istituto Nazionale di Fisica Nucleare, University and Scuola Normale Superiore of Pisa, I-56100 Pisa, Italy*

[45] *University of Pittsburgh, Pittsburgh, Pennsylvania 15260*

[46] *Purdue University, West Lafayette, Indiana 47907*

[47] *University of Rochester, Rochester, New York 14627*

[48] *The Rockefeller University, New York, New York 10021*

[49] *Istituto Nazionale di Fisica Nucleare, Sezione di Roma 1, University di Roma "La Sapienza," I-00185 Roma, Italy*

[50] *Rutgers University, Piscataway, New Jersey 08855*

[51] *Texas A&M University, College Station, Texas 77843*

[52] *Texas Tech University, Lubbock, Texas 79409*

[53] *Istituto Nazionale di Fisica Nucleare, University of Trieste/ Udine, Italy*

[54] *University of Tsukuba, Tsukuba, Ibaraki 305, Japan*

[55] *Tufts University, Medford, Massachusetts 02155*

5

[56] *Waseda University, Tokyo 169, Japan*

[57] *Wayne State University, Detroit, Michigan 48201*

[58] *University of Wisconsin, Madison, Wisconsin 53706*

[59] *Yale University, New Haven, Connecticut 06520*

We present the results of a search for doubly-charged Higgs bosons ($H^{\pm\pm}$) decaying to dileptons using ≈ 240 pb^{-1} of $p\bar{p}$ collision data collected by the CDF II experiment at the Fermilab Tevatron. In our search region, given by same-sign dilepton mass $m_{ll'} > 80$ GeV/c^2 (100 GeV/c^2 for dielectron channel), we observe no evidence for doubly-charged Higgs production. We set limits on $\sigma(p\bar{p} \to H^{++}H^{--} \to l^+l^+l^-l^-)$ as a function of the mass of the doubly-charged Higgs boson and the chirality of its couplings. Assuming exclusive same-sign dilepton decays, we derive lower mass limits on $H^{\pm\pm}_L$ of 133 GeV/c^2, 136 GeV/c^2, and 115 GeV/c^2 in the ee, $\mu\mu$, and $e\mu$ channels, respectively, and a lower mass limit of 113 GeV/c^2 on $H^{\pm\pm}_R$ in the $\mu\mu$ channel, all at the 95% confidence level.

The standard model (SM) gives a good description of the known fundamental particles, using the $SU(3)_C \times SU(2)_L \times U(1)_Y$ gauge group to describe their non-gravitational interactions. The $SU(2)_L \times U(1)_Y$ electroweak gauge symmetry is broken to $U(1)_{EM}$ by the Higgs mechanism, but a Higgs boson has yet to be observed. The observation of any Higgs particle would be an important step toward understanding the physics at the electroweak scale. In addition to the SM $SU(2)_L$ Higgs doublet, a number of models [1–3] predict new Higgs doublets or triplets containing doubly-charged Higgs bosons ($H^{\pm\pm}$). For example, the left-right symmetric model [2], predicated on a right-handed version of the weak force $SU(2)_R$, requires a Higgs triplet. The model predicts light neutrino masses by the seesaw mechanism [4], consistent with recent data on neutrino oscillations [5]. Furthermore, the left-right symmetric model suggests light ($\mathcal{O}(100 \text{ GeV}/c^2)$) doubly-charged Higgs particles if supersymmetry is a property of nature [3], and is therefore of interest for direct searches at high-energy colliders.

Doubly-charged Higgs bosons couple directly to leptons, photons, W and Z bosons, and singly-charged Higgs bosons ($H^{\pm}$). The $H_L^{\pm\pm}$ and $H_R^{\pm\pm}$ bosons respectively couple to left- and right-handed particles, and may have different fermionic couplings. Their coupling to a pair of W bosons is experimentally constrained to be small due to the small observed value of $|\rho_{EW} - 1|$ [6], resulting in a negligible cross section for the process $p\bar{p} \to W^{\pm} \to W^{\mp}H^{\pm\pm}$. Therefore, $H^{\pm\pm}$ production would be dominated by the reaction $p\bar{p} \to Z/\gamma^* \to H^{++}H^{--}$, whose cross section is independent of the $H^{\pm\pm}$ fermionic couplings.

The $H^{\pm\pm}$ decays predominantly to charged leptons if $m_{H^{\pm\pm}} < 2m_{H^{\pm}}$ and $m_{H^{\pm\pm}} - m_{H^{\pm}} < m_{W^{\pm}}$ [7]. The leptonic decays conserve the quantum number $B - L$, where B is baryon number and L is lepton number. The $H^{\pm\pm}$ couplings $h_{ll'}$ to electrons and muons are experimentally constrained by the absence of $H^{\pm\pm}$ production in e^+e^- collisions ($h_{ee} < 0.07$) [8], and the non-observation of the decays $\mu \to 3e$ ($h_{ee}h_{e\mu} < 3.2 \times 10^{-7}$) and $\mu \to e\gamma$ ($h_{\mu\mu}h_{e\mu} < 2 \times 10^{-6}$) [9]. The experimental constraints on the couplings (quoted here for $m_{H^{\pm\pm}} = 100 \text{ GeV}/c^2$) weaken with increasing doubly-charged Higgs mass. The $h_{\mu\mu}$ coupling is probed by measurements of the anomalous magnetic moment of the muon $(g-2)_\mu$; the previous limit $h_{\mu\mu} < 0.25$ [9] has not been reanalyzed using the most recent $(g-2)_\mu$ measurement [10].

Direct searches by the OPAL and L3 collaborations in e^+e^- collisions [11] have excluded doubly-charged Higgs bosons below masses of about 100 GeV/c^2, assuming exclusive $H^{\pm\pm}$ decay to a given dilepton channel. A recent search by the DØ collaboration in the $\mu\mu$ channel [12] has excluded $H_L^{\pm\pm}$ below a mass of 118 GeV/c^2. In this Letter, we describe a search for doubly-charged resonances in the same-sign ee, $e\mu$, and $\mu\mu$ channels, using ≈ 240 pb^{-1} [13]

of data collected at $\sqrt{s} = 1.96$ TeV by the CDF II experiment at the Fermilab Tevatron. We present our results using the doubly-charged Higgs production model [4], and set the world's highest mass limits in the electron and muon channels. We probe the range of coupling $10^{-5} < h_{ll'} < 0.5$, which corresponds to narrow resonances that decay promptly ($c\tau < 10$ μm, where τ is the lifetime).

The CDF II detector [14] consists of three major subsystems: an inner tracking detector, a lead (iron) scintillator sampling calorimeter for measuring electromagnetic (hadronic) showers, and outer drift chambers for muon identification. The inner detector includes a high-resolution wire chamber (the Central Outer Tracker, or COT [15]) which, along with the central calorimeter and muon system, covers the pseudorapidity interval $| \eta | < 1$ [16].

Our strategy is to search for one of the pair-produced $H^{\pm\pm}$ bosons to maximize the sensitivity, and to permit detection of any singly-produced doubly-charged resonance. The event triggers can be classified by the requirements of (1) two energy clusters with $E_T > 18$ GeV in the electromagnetic calorimeter (2EM), (2) a central electromagnetic cluster with $E_T > 18$ GeV and matching track $p_T > 9$ GeV/c (1EM), or (3) a COT track with $p_T > 18$ GeV/c with an associated track segment ("stub") in the muon detectors.

The same-sign ee sample is selected primarily using the 2EM trigger. In the offline analysis, we require two same-sign central electrons with calorimeter $E_T > 30$ GeV and COT track $p_T > 10$ GeV/c. Electrons are identified using the ratio of calorimeter energy (E) to track momentum (p) ($\frac{E}{pc} < 4$), longitudinal and lateral shower profiles, track-cluster matching, calorimeter isolation energy in a surrounding cone, and photon-conversion identification using the tracker. The same-sign ee sample corresponds to an integrated luminosity of (235 ± 13) pb^{-1}. The luminosity is determined by measuring the rate of inelastic collisions, and the uncertainty has equal contributions from the uncertainty on the inelastic cross section and the uncertainty on the acceptance of the luminosity counters.

The same-sign $\mu\mu$ sample is selected using the single-muon trigger, with a consistent offline requirement of a matching stub. We select tracks with $p_T > 25$ GeV/c that are minimum-ionizing, $i.e.$ have small electromagnetic and hadronic energy depositions in the calorimeters. The cosmic-ray muon background is suppressed by requiring the muons to originate from the beam line, to be coincident in time with each other and with a $p\bar{p}$ collision, and to be consistent with a pair of outgoing particles [17]. Track-quality requirements and calorimeter isolation suppress hadronic-jet backgrounds. The integrated luminosity of the same-sign $\mu\mu$ sample is (242 ± 14) pb^{-1}.

The same-sign $e\mu$ sample is selected mainly using the 1EM trigger. We require a central electron and a track matched to a muon stub. The stub requirement significantly reduces background, but also reduces the fiducial

acceptance of $H^{\pm\pm} \to e\mu$ relative to the $\mu\mu$ and ee samples. The integrated luminosity of the same-sign $e\mu$ sample is (240 ± 14) pb^{-1}. All electron and muon tracks are constrained to the transverse position of the beam to improve their momentum resolution.

We calculate trigger efficiencies using separate unbiased triggers, the tracking efficiency using $Z \to ee$ events, and the lepton-identification efficiencies with $Z \to ee/\mu\mu$ events. We obtain $(96.6 \pm 0.4)\%$ and $(100.00^{+0.00}_{-0.02})\%$ as the efficiencies of the 1EM and 2EM triggers, respectively. The muon trigger efficiencies, including the offline matching-stub requirement, are $(77.1 \pm 1.3)\%$ and $(93.9 \pm 0.8)\%$ for $|\eta| < 0.6$ and $0.6 < |\eta| < 1$, respectively, each corresponding to a separate detector subsystem. The tracking algorithm is highly efficient ($> 99\%$) for isolated charged particles within the COT fiducial volume. The lepton-identification efficiencies are $(92.7 \pm 0.3)\%$ and $(90.8 \pm 0.2)\%$ for electrons and muons, respectively. The corresponding efficiencies measured in simulated [19] Z events are $(89.3 \pm 0.1)\%$ and $(91.3 \pm 0.1)\%$. The simulated $H^{\pm\pm}$ detection efficiency is corrected by the ratio of data to simulated Z boson efficiencies.

The potential backgrounds from SM processes are (1) hadrons that decay to leptons or are misidentified as such, (2) leptonic decays of W bosons, produced in association with hadronic jet(s) (W+jet), (3) Z/γ^* decays (Drell-Yan), where the same-sign track comes from a photon conversion, (4) WZ production, where both the W and Z decay leptonically, and (5) cosmic rays.

The hadronic background is estimated using lepton-triggered events with two same-sign lepton candidates [18], each failing the identification requirements ("failing lepton candidate"). The ratio of the number of lepton candidates passing to the number failing the requirements (the "pass-fail ratio") is measured using jet data samples. These samples are selected either using high-E_T (> 100 GeV) or low-E_T (> 20 GeV) jet triggers, or using single-lepton triggers and excluding leptonic W and Z decays. The pass-fail ratio is $\mathcal{O}(0.05)$, with a systematic uncertainty of $\approx 80\%$ arising from its sample dependence. It is used to apply a weight to each candidate lepton (as a function of E_T) in events with two failing lepton candidates to obtain the dilepton mass distribution.

The W+jet background is determined by applying the pass-fail ratio as a weight to W data events which have a second failing lepton and $25 < \not{E}_T < 60$ GeV. The expected misidentified-W contribution (from jets) is subtracted to prevent double-counting. We use simulated [19] W+jet events to correct for the acceptance of the $\not{E}_T$ requirement. Background from $W\gamma$ production, where the photon converts to an e^+e^- pair, is implicitly included in this estimate. It is studied explicitly using the simulation and found to be negligible.

Background from $Z/\gamma^* \to e^+e^-$ occurs when one electron radiates a photon which subsequently converts to an
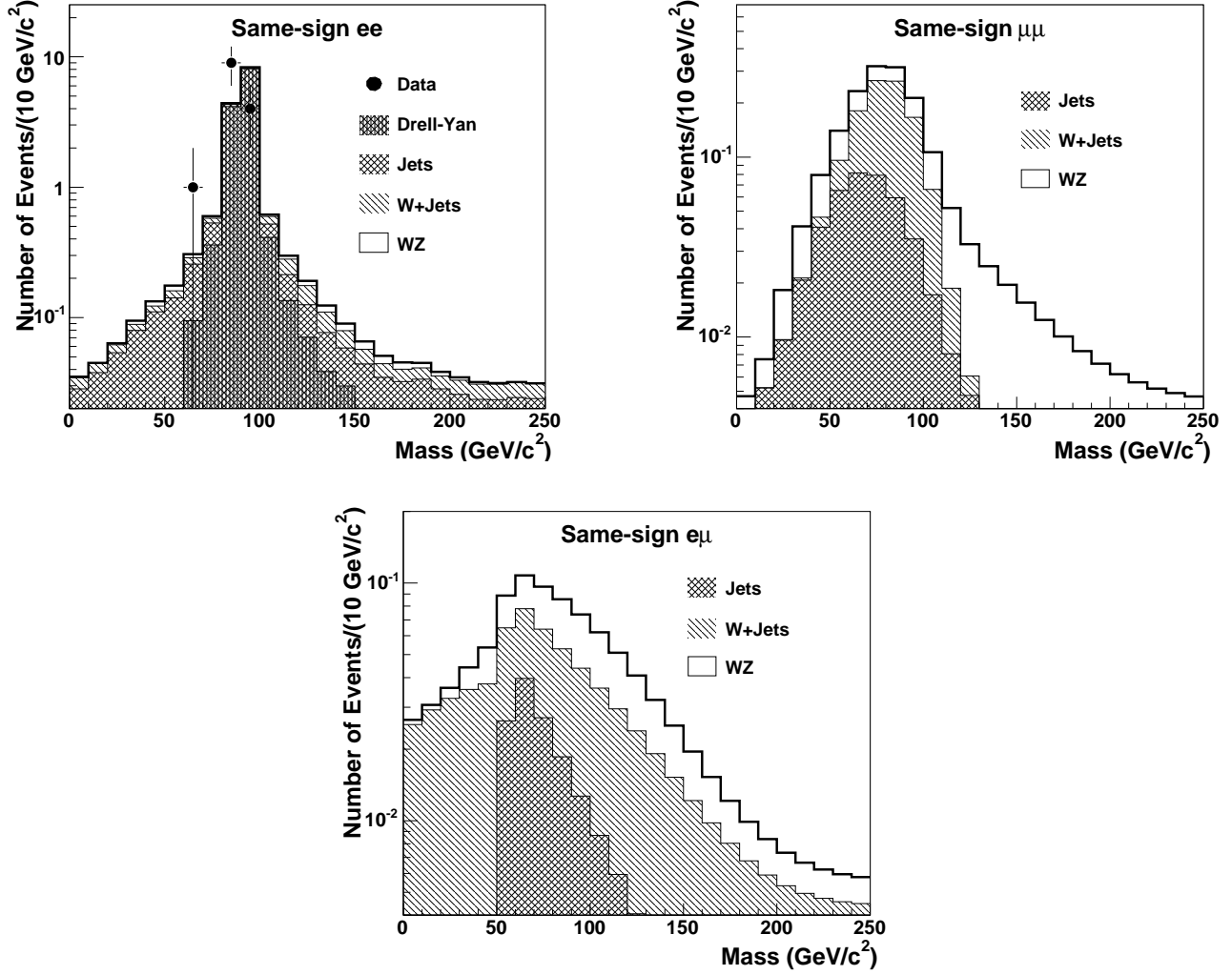
FIG. 1. The same-sign dilepton mass distributions of the ee data and the cumulative SM contributions to the ee (top-left), $\mu\mu$ (top-right), and $e\mu$ (bottom) samples. The solid line is the overall sum of the indicated areas. No same-sign $\mu\mu$ or $e\mu$ events are observed.

e^+e^- pair. When a same-sign conversion electron has higher momentum than the prompt electron and is associated with the cluster, the event is reconstructed with two same-sign electrons. The mass dependence is obtained from simulated [19] Drell-Yan events. The simulated sample is normalized using the number of same-sign candidates in the Z mass region (80 GeV/c^2 < m_{ee} < 100 GeV/c^2), after subtracting jet and W+jet contributions.

Background from $WZ \rightarrow l\nu ll$ production is estimated using simulation [19]. We use the next-to-next-to-leading order production cross section of 4.0 pb [23], and apply the trigger, tracking, and lepton-identification efficiencies to the events that pass the kinematic and geometric selection.

The cosmic-ray background is estimated using COT timing information. We use an independently identified sample

of cosmic rays to estimate the residual contribution surviving the timing requirements made in the $\mu\mu$ analysis. The expected cosmic-ray background is found to be 0.02 ± 0.02 events, which we take to be negligible.

Background	Low-Mass Region	High-Mass Region
$Z/\gamma^* \to ee$	0.46 ± 0.13	0.37 ± 0.11
Jets$\to ee$	$0.47^{+0.23}_{-0.19}$	$0.62^{+0.71}_{-0.44}$
W+jet$\to ee$	0.14 ± 0.08	0.36 ± 0.21
$WZ \to ee$	0.07 ± 0.02	0.11 ± 0.03
Total ee	1.1 ± 0.4	$1.5^{+0.9}_{-0.6}$
Jets$\to \mu\mu$	$0.30^{+0.24}_{-0.16}$	$0.19^{+0.35}_{-0.17}$
W+jet$\to \mu\mu$	0.32 ± 0.22	0.40 ± 0.27
$WZ \to \mu\mu$	0.21 ± 0.04	0.19 ± 0.03
Total $\mu\mu$	0.8 ± 0.4	$0.8^{+0.5}_{-0.4}$
Jets$\to e\mu$	0.09 ± 0.05	0.06 ± 0.05
W+jet$\to e\mu$	$0.22^{+0.24}_{-0.15}$	0.25 ± 0.17
$WZ \to e\mu$	0.12 ± 0.02	0.12 ± 0.03
Total $e\mu$	0.4 ± 0.2	0.4 ± 0.2

TABLE I. The integrated background for the ee, $\mu\mu$ and $e\mu$ samples for the low-mass (< 80 GeV/c^2) and high-mass (100-300 GeV/c^2 for ee, 80-300 GeV/c^2 for $\mu\mu$ and $e\mu$) regions.

Figure 1 shows the total background and the data as a function of $m_{ll'}$ for each sample. The predominantly back-to-back lepton topologies, the kinematic thresholds, and the typical lepton p_T from W or Z decays lead to the observed peaked shapes of the background distributions. The search is performed in the region of $m_{ll'} > 80$ GeV/c^2 for the $\mu\mu$ and $e\mu$ samples, and in the region of $m_{ee} > 100$ GeV/c^2 for the ee sample. The low-mass regions ($m_{ll'} < 80$ GeV/c^2) are used to check our background predictions. Table I summarizes the total background predictions. We estimate 1.1 ± 0.4 (ee), 0.8 ± 0.4 ($\mu\mu$), and 0.4 ± 0.2 ($e\mu$) events in the low-mass regions, and observe one ee event ($m_{ee} = 70$ GeV/c^2) and no $\mu\mu$ or $e\mu$ events. As an additional check, we compare the predicted and observed backgrounds for same-sign dilepton events with one failing lepton candidate and $\not{E}_T < 15$ GeV. The expectations of 54 ± 21 (ee), 7.6 ± 3.1 ($\mu\mu$), and 2.4 ± 0.8 ($e\mu$) events are consistent with the observed numbers of 63 (ee), 8 ($\mu\mu$), and 2 ($e\mu$) events.

The same-sign dilepton mass resolution is $\approx 3.5\%$ of the mass. The intrinsic $H^{\pm\pm}$ width is equal to $h^2_{ll'} m_{H^{\pm\pm}}/8\pi$ [6], and contributes negligibly to the reconstructed mass. We define search windows of $\pm10\%$ of a given $H^{\pm\pm}$ mass, corresponding to a $\pm3\sigma$ window. We predict the acceptances as a function of $H^{\pm\pm}$ mass using the simulation [19], including the efficiency scale factors. The acceptance systematic uncertainty is dominated by the parton distribution function uncertainty, which we estimate to be 4% using the MRST prescription [24]. In the mass range of interest, the acceptances are $\approx 34\%$ for the ee and $\mu\mu$ channels and $\approx 18\%$ for the $e\mu$ channel.
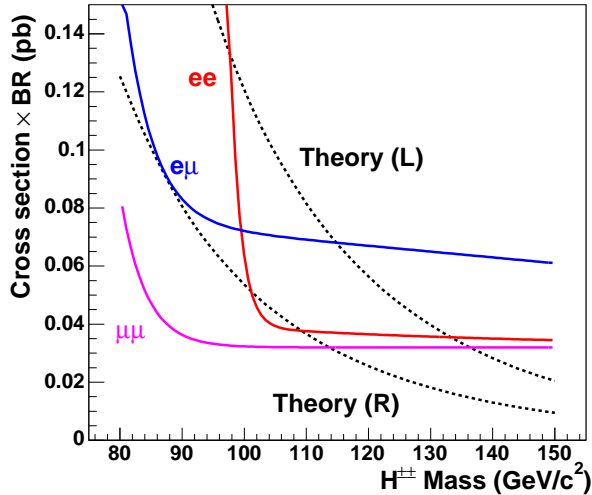
FIG. 2. Experimental limits on cross section × branching ratio at 95% C.L. as a function of doubly-charged Higgs mass (solid curves). Dotted curves show the theoretical next-to-leading order total cross sections [26] for left-handed and right-handed $H^{\pm\pm}$ couplings.

No events are found in the high-mass regions of the ee, $\mu\mu$ and $e\mu$ samples. This null result yields a 95% confidence level (C.L.) upper limit on the cross section as a function of doubly-charged Higgs mass (Fig. 2). We calculate the limit using a Bayesian method [25] with a flat prior for the signal and Gaussian priors for background and acceptance uncertainties. Through comparison with the theoretical cross sections [26], we obtain mass limits of 133 GeV/c^2, 136 GeV/c^2, and 115 GeV/c^2, for exclusive $H_L^{\pm\pm}$ decays to ee, $\mu\mu$, and $e\mu$, respectively, and 113 GeV/c^2 for exclusive $H_R^{\pm\pm}$ decays to $\mu\mu$. Figure 3 shows these results in the mass-coupling plane, along with the current world limits.

In summary, we have performed an inclusive search for doubly-charged resonances in same-sign ee data with $m_{ee} > 100$ GeV/c^2, and same-sign $\mu\mu$ and $e\mu$ data with $m_{ll'} > 80$ GeV/c^2. We have found no evidence for new doubly-charged resonances, and have significantly extended the existing mass limits on doubly-charged Higgs bosons decaying exclusively to ee ($m_{H_L^{\pm\pm}} > 133$ GeV/c^2), $\mu\mu$ ($m_{H_L^{\pm\pm}} > 136$ GeV/c^2 and $m_{H_R^{\pm\pm}} > 113$ GeV/c^2), or $e\mu$ ($m_{H_L^{\pm\pm}} > 115$ GeV/c^2) final states.
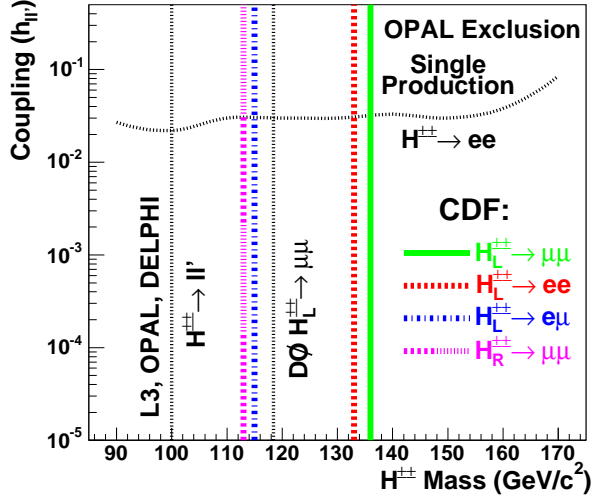
FIG. 3. The doubly-charged Higgs lower mass limits versus lepton coupling $(h_{ll'})$ from this analysis, assuming exclusive decay to a given dilepton pair. Our limits are valid for $h_{ll'} > 10^{-5}$. Previous limits [8,11,12] are also shown.

[1] T. P. Cheng and L.-F. Li, Phys. Rev. D**22**, 2860 (1980).

[2] R. N. Mohapatra and J. C. Pati, Phys. Rev. D**11**, 566 (1975).; G. Senjanovic and R. N. Mohapatra, Phys. Rev. D**12**, 1502 (1975); R. N. Mohapatra and G. Senjanovic, Phys. Rev. D**23**, 165 (1981).

[3] C. S. Aulakh, A. Melfo, and G. Senjanovic, Phys. Rev. D**57**, 4174 (1998); Z. Chacko and R. N. Mohapatra, Phys. Rev. D**58**, 015003 (1998).

[4] R. N. Mohapatra and G. Senjanovic, Phys. Rev. Lett. **44**, 912 (1980).

[5] Super-Kamiokande Collaboration, Y. Ashie *et al.*, hep-ex/0404034 (submitted to Phys. Rev. Lett.) and references therein.

[6] J. F. Gunion *et al.*, Phys. Rev. D**40**, 1546 (1989). The parameter ρ_{EW} is defined as $m^2_{W_L}/(m^2_Z \cos^2 \theta_W)$.

[7] $H^{\pm}$ mass below ≈ 80 GeV has been excluded at the 95% C.L. using $\tau\nu_\tau$ and $c\bar{s}$ decay channels, see DELPHI Collaboration, J. Abdallah *et al.*, Eur. Phys. J. C**34**, 399 (2004); L3 Collaboration, P. Achard *et al.*, Phys. Lett. B**575**, 208 (2003); ALEPH Collaboration, A. Heister *et al.*, Phys. Lett. B**543**, 1 (2002).

[8] OPAL Collaboration, G. Abbiendi *et al.*, Phys. Lett. B**577**, 93 (2003).

[9] R. N. Mohapatra, Phys. Rev. D**46**, 2990 (1992).

[10] Muon (g-2) Collaboration, G. W. Bennett *et al.*, Phys. Rev. Lett. **92**, 161802 (2004).

[11] DELPHI Collaboration, J. Abdallah *et al.*, Phys. Lett. B**552**, 127 (2003); OPAL Collaboration, G. Abbiendi *et al.*, Phys. Lett. B**526**, 221 (2002); L3 Collaboration, P. Achard *el al.*, Phys. Lett. B**576**, 18 (2003).

[12] DØ Collaboration, V. M. Abazov *et al.*, hep-ex/0404015 (submitted to Phys. Rev. Lett.).

[13] S. Klimenko, J. Konigsberg, and T. M. Liss, Fermilab-FN-0741 (unpublished).

[14] CDF II Collaboration, R. Blair *et al.*, Fermilab-Pub-96-390-E.

[15] T. Affolder *et al.*, Nucl. Instrum. Meth. Phys. Res. A **526**, 249 (2004).

[16] CDF uses a cylindrical coordinate system in which ϕ is the azimuthal angle, r is the radius from the nominal beamline, and $+z$ points in the direction of the proton beam and is zero at the center of the detector. The pseudorapidity $\eta = -\ln[\tan(\theta/2)]$, where θ is the polar angle with respect to the z axis. Calorimeter energy (track momentum) measured transverse to the beam is denoted as E_T (p_T), and the total calorimetric transverse energy imbalance is denoted as $\not{E}_T$.

[17] A. V. Kotwal, H. K. Gerberich and C. Hays, Nucl. Instrum. Meth. Phys. Res. A **506**, 110 (2003).

[18] Electron candidates are EM clusters with $E_T > 25$ GeV and matching track $p_T > 10$ GeV/c, and muon candidates are tracks with $p_T > 20$ GeV/c.

[19] All simulated samples are generated with PYTHIA [20] and use a detector simulation based on GEANT [21].

[20] T. Sjöstrand, Comput. Phys. Commun. **82**, 74 (1994). We used version 6.127.

[21] R. Brun and F. Carminati, CERN Program Library Long Writeup, W5013, 1993 (unpublished). We used version 3.15.

[22] M. L. Mangano *et al.*, JHEP **0307**, 001 (2003).

[23] J. M. Campbell and R. K. Ellis, Phys. Rev. D**60**, 113006 (1999).

[24] A. D. Martin, R. G. Roberts, W. J. Stirling and R. S. Thorne, Eur. Phys. J. C **4**, 463 (1998); Eur. Phys. J. C **23**, 73 (2002).

[25] I. Bertram *et al.*, Fermilab-TM-2104 (unpublished); J. Conway, CERN 2000-005, 247 (2000); K. Hagiwara *et al.*, Phys. Rev. D**66**, 010001 (2002), section 31. The posterior likelihood is rendered normalizable by introducing a reasonably large cutoff.

[26] M. Mühlleitner and M. Spira, Phys. Rev. D**68**, 117701 (2003). The cross sections have theoretical uncertainties of (5-10)%.